Roiz, Mikhail; Kumar, Krishna; Karhu, Juho; Vainio, Markku

Simple method for mid-infrared optical frequency comb generation with dynamic offset
frequency tuning

Simple method for mid-infrared optical frequency comb generation with dynamic offset frequency tuning

Mikhail Roiz, Krishna Kumar, Juho Karhu, and Markku Vainio

COLLECTIONS

F   This paper was selected as Featured

View Online   Export Citation   CrossMark

ARTICLES YOU MAY BE INTERESTED IN

Hybrid InP and SiN integration of an octave-spanning frequency comb
APL Photonics **6**, 026102 (2021); https://doi.org/10.1063/5.0035452

Simple single-section diode frequency combs
APL Photonics **5**, 121303 (2020); https://doi.org/10.1063/5.0033211

Controlling the direction of topological transport in a non–Hermitian time-reversal symmetric Floquet ladder
APL Photonics **6**, 010801 (2021); https://doi.org/10.1063/5.0036494

Simple method for mid-infrared optical frequency comb generation with dynamic offset frequency tuning Ⓕ

View Online   Export Citation   CrossMark

Mikhail Roiz,[1,a] ⓘD Krishna Kumar,[1] Juho Karhu,[1,2] ⓘD and Markku Vainio[1,3,a] ⓘD

AFFILIATIONS

[1] Department of Chemistry, University of Helsinki, FI-00560 Helsinki, Finland
[2] Metrology Research Institute, Aalto University, Espoo FI-00076, Finland
[3] Photonics Laboratory, Physics Unit, Tampere University, Tampere FI-33101, Finland

[a] Authors to whom correspondence should be addressed: mikhail.roiz@helsinki.fi and markku.vainio@helsinki.fi

ABSTRACT

We present a simple method for fully stabilized mid-infrared optical frequency comb generation based on single-pass femtosecond optical parametric generation that is seeded by a continuous-wave laser. We have implemented the method in a periodically poled lithium niobate crystal that produces a frequency comb tunable across 3325 nm–4000 nm ($2380\,cm^{-1}$–$3030\,cm^{-1}$). The method generates the mid-infrared (idler) comb with known and stabilized Carrier-Envelope Offset (CEO) frequency without the need to directly detect it. The idler CEO is continuously tunable for almost half of the repetition rate and can be modulated. Together with the high output power (up to 700 mW) and low intensity noise (0.018% integrated in 10 Hz–2 MHz bandwidth), this makes the demonstrated mid-infrared frequency comb promising for many applications such as high-precision molecular spectroscopy, frequency metrology, and high harmonic generation.

I. INTRODUCTION

Since their first development about 20 years ago, Optical Frequency Combs (OFCs) have advanced science and technology in many different ways. By creating a phase-coherent link between optical and radio frequencies,[1] OFCs have enabled accurate measurements of optical frequencies with a simple and elegant implementation leading to rapid progress in the development of new optical frequency standards.[2] The establishment of OFCs has only become possible thanks to the invention of novel techniques for precise measurement and control of Carrier-Envelope Offset (CEO) frequency—a key parameter for ensuring pulse-to-pulse coherence in femtosecond Mode Locked Lasers (MLLs).[3,4] Consequently, OFCs have found applications in a variety of different fields[5–7] including optical atomic clocks,[8] optical arbitrary waveform generators,[9] precise ranging, telecommunications, and molecular spectroscopy.[10,11]

Despite the fact that MLL technology opened up a new path to high-precision molecular spectroscopy, a major challenge has been to access the Mid-Infrared (MIR) spectral region, where a variety of strong molecular fingerprints can be measured.[10,12] Although many alternative techniques for MIR OFC generation were proposed, including direct MIR OFC generation by quantum cascade lasers,[13] in general it requires nonlinear frequency conversion processes to be involved. The two most common methods for MIR OFC generation based on nonlinear conversion are Difference Frequency Generation (DFG) and Synchronously Pumped Optical Parametric Oscillation (SPOPO). In most cases, DFG requires either two fully stabilized Near-Infrared (NIR) OFCs for the input[14] or one NIR OFC and its extended version via supercontinuum (SC) generation.[15–19] While the second option of DFG allows one to use a single NIR comb for the pump and signal, this implementation leads to cancellation of CEO (it is always 0 for the MIR comb), and thus, the CEO cannot be changed easily. On the other hand, one of the DFG methods involves mixing of a CW pump laser with an NIR OFC, in which case the CEO can be precisely controlled by varying the pump laser frequency.[20,21] The drawbacks of this approach are low MIR output power and a rather complicated experimental setup. SPOPO does not make the CEO tuning easier, since for a singly resonant SPOPO, one needs to precisely control the pump CEO and

the cavity length at the same time to tune the MIR comb CEO, and determination of the exact CEO frequency requires an additional measurement setup.[12,22,23] In doubly resonant degenerate SPOPO,[24] the CEO tuning can be performed just by tuning the CEO of the pump laser, but this scheme implies the random choice between two possible CEO values for the MIR comb,[23,25–27] complicating its CEO determination. In addition, SPOPOs generally require precise cavity locking[28] and careful engineering of the group delay dispersion.[25]

In the present work, we demonstrate a simple approach for the generation of fully stabilized MIR OFCs with CEO tuning and modulation. The approach is based on single-pass femtosecond Optical Parametric Generation (OPG) seeded by a continuous-wave (CW) laser, and it can be applied to any OPG. Importantly, OPG on its own does not directly lead to the generation of stable OFCs for the signal and idler, since the process starts from noise, and thus, the CEO is random for two subsequent signal and idler pulses. In order to fully stabilize the output MIR comb, we use a CW laser phase-locked to the pump laser to seed the signal comb. Several important advantages arise here compared to DFG and SPOPO. First, the idler CEO is defined by the radio-frequency (RF) local oscillator (LO) used for phase-locking of the seed laser, which means that there is no need to measure the CEO, since it is always known. Second, the CEO of the MIR comb is continuously tunable by simply changing the RF LO frequency. It makes the system highly versatile combined with easily tunable repetition rate thanks to the cavity free design. Third, the idler CEO can also be modulated at relatively high frequencies precisely maintaining its CEO central frequency. Moreover, the method is inherently free of any optical self-referencing techniques like f-2f[4,5] and 2f-3f[29] interferometry meaning that the CEO of the pump MLL can be left free running. We believe that the presented simple method for the generation of fully stabilized MIR OFCs has major advantages compared to the existing methods, especially in applications that require precise control of the CEO and repetition rate, such as cavity enhanced spectroscopy,[30] dual-comb spectroscopy,[31–33] comb-assisted spectroscopy,[34,35] and high harmonic generation.[36,37] Additionally, the setup demonstrated here can be used as a pump source for another OPG, DFG, or SPOPO,[38] since it has a large wavelength tuning range and high output power. The high output power is also vital for certain spectroscopic methods including OFC photoacoustic spectroscopy[39,40] and background-free absorption spectroscopy.[41] In this article, we demonstrate the proof of concept implementation of the method, including rigorous characterization of the system.

II. PRINCIPLE

Usually, in OPG, high-energy pulses are used to pump a nonlinear crystal, which in the non-degenerate case leads to the generation of signal and idler pulses. The generation of the new pulses is governed by the quantum noise amplification. This makes the process inefficient and leads to loss of pulse-to-pulse coherence of the produced signal and idler pulse trains. The situation changes if the OPG is seeded by an additional light source in the signal or idler spectral region, which is similar to Optical Parametric Amplifiers (OPAs). First, the seeding may lead to a significant reduction of the OPG threshold.[42] Second, it improves the pulse-to-pulse coherence provided that the seeding source is coherent.[19] Third, it reduces the

relative intensity noise (RIN) of the system,[43] which is vital for many spectroscopy applications. In addition, it was demonstrated that two OPG setups seeded by the same CW seed laser produce mutually coherent output NIR combs (signal), which is useful for dual-comb spectroscopy.[44] Despite all the benefits, to the best of our knowledge, the possibility of using CW-seeded OPG to produce a fully stabilized MIR OFC source has not been demonstrated before.

Numerous OPG and OPA experiments have been reported using different nonlinear materials including BBO,[45] PPKTP,[46] GaAs,[47] and LiTaO₃.[48] Of particular interest is the OPG in MgO doped periodically poled lithium niobate (MgO:PPLN) because this crystal has a high nonlinear coefficient, high damage threshold, and large transparency range that extends to the 3 μm CH-stretching vibrational region, which is useful for molecular spectroscopy. Importantly, when the pump source has a pulse duration in the range of hundreds of femtoseconds or less, the interaction length may become an issue. Due to the differences in group velocities between the pump, signal, and idler pulses, the interaction length can be so short that the OPG threshold is never reached without the risk of damaging the crystal. This is a general problem for all nonlinear crystals pumped by ultrashort pulses, but, fortunately, several research groups demonstrated that MgO:PPLN supports a special case of OPG where the interaction length can be as long as 50 mm leading to conversion efficiencies over 50% with low threshold.[49,50] A distinctive feature of this particular case is the convenient pump wavelength of 1030 nm–1064 nm that coincides with the mature technology of high power Nd:YAG solid state and Yb-doped fiber MLLs. When launched into the MgO:PPLN in the given spectral range, the high-energy pump generates the signal and idler pulses, whose group velocities have opposite signs and equal absolute values leading to a so-called pulse trapping effect.[51]

In general, each optical frequency component ν_n of a frequency comb can be represented as a combination of two radio frequencies using the following formula:[5]

$$\nu_n = f_{CEO} + n f_r,$$

where f_r is the repetition rate, f_{CEO} is the CEO frequency, and n is the mode number of the given optical frequency components (comb tooth). We will use CEO instead of f_{CEO} further in the text. As usual, f_r is directly detectable using a fast photodiode and, thus, easy to stabilize. On the other hand, CEO cannot be directly detected without an additional measurements setup, such as an f-2f interferometer.[4] Luckily, in OPG, there is a way to determine, stabilize, and freely tune the idler CEO without directly detecting it.

Considering the principle of conservation of energy, the CEO equation for the OPG process can be written as follows:

$$CEO_p = CEO_s + CEO_i, \tag{1}$$

where CEO_p, CEO_s, and CEO_i are the offset frequencies of the pump, signal, and idler combs, respectively. In regular OPG without seeding, even if the CEO_p is stabilized, CEO_s and CEO_i are random. On the contrary, if one seeds the signal comb with a coherent source, the CEO_s follows the seed source, which consequently leads to a change in CEO_i to satisfy Eq. (1). We can use this feature in our favor to stabilize the CEO_i. Let us first assume that $CEO_s = CEO_p$; according to Eq. (1), it leads to $CEO_i = 0$, which is the case of DFG mentioned above.[15,16] Here, it does not matter whether the CEO_p is stabilized

or not because the CEO_i will always remain zero, thanks to Eq. (1). Next, let us set the CEO_s in a different way,
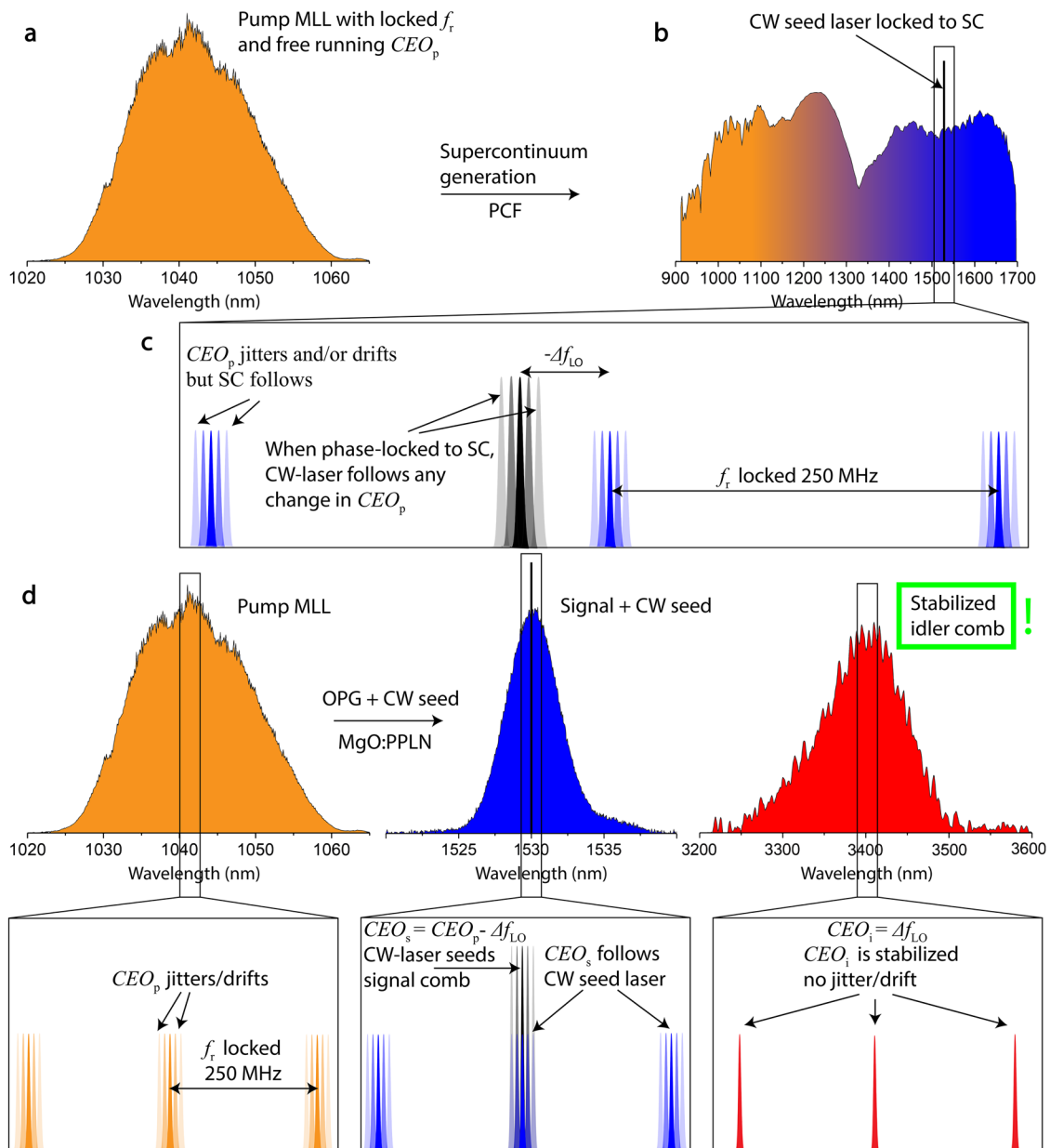
$$CEO_s = CEO_p - \Delta f \qquad (2)$$

or

$$CEO_s = CEO_p + \Delta f, \qquad (3)$$

where Δf is a frequency offset; in this case, we have two states, $CEO_i = \Delta f$ or $CEO_i = -\Delta f$, respectively, for Eqs. (2) and (3), which are easy to distinguish in our setup. Hence, if one can precisely set Δf, it means that CEO_i is known and freely tunable.

In practice, the above-mentioned CEO_i stabilization can be performed in the four steps schematically shown in Fig. 1. First, the output beam of the pump MLL is split into two arms. Note that in order to produce fully stabilized MIR comb, repetition rate of the

**FIG. 1.** Schematic of the CW seeded OPG for stabilized MIR OFC generation. (a) Pump optical spectrum. (b) SC optical spectrum combined with CW seed laser. (c) CW seed laser (black line) locked to SC (blue lines) in the state corresponding to Eq. (2): $CEO_s = CEO_p - \Delta f_{LO}$. (d) Generated signal and idler spectra using CW seeded OPG (above) and the schematic of the corresponding laser modes (below).

pump MLL should be stabilized (CEO_p can be left free running). Second, the first arm is used to generate SC that reaches the CW seed laser wavelength (see "supplementary material note 1: Supercontinuum generation" for details). Third, the CW seed laser frequency is phase-locked to the generated SC. When phase-locking is performed, the frequency offset Δf is defined by an RF LO, which is why we denote $\Delta f = \Delta f_{LO}$; see "supplementary material note 2: Phase-locking" for more information. Since Δf_{LO} can be easily changed, the CEO_i is continuously tunable. On the last step, the second arm of the pump MLL and the phase-locked CW seed laser are combined in a nonlinear crystal and used to generate the signal and idler combs via seeded OPG.

By phase-locking the CW seed laser to the SC produced from the pump MLL, we transfer all the changes and fluctuations of the CEO_p to CEO_s, which according to Eq. (1) makes the CEO_i stable. Note that in Fig. 1, we only consider the case of Eq. (2) that corresponds to $CEO_i = \Delta f_{LO}$. The states in Eqs. (2) and (3) can be distinguished in the phase-locking process by simply monitoring the behavior of the RF beat note between the CW seed laser and the SC. The state of Eq. (2) is realized when prior to locking the RF beat note frequency decreases while increasing the optical CW laser frequency (decreasing wavelength); if the opposite is true, then the state corresponding to Eq. (3) is realized. All the optical spectra in Figs. 1(a), 1(b), and 1(d) are examples of real measured spectra. The spectra are shown in a linear scale with arbitrary units except for the SC spectrum in Fig. 1(b), which is shown in the decibel logarithmic scale for clarity (see "supplementary material note 1: Supercontinuum generation" for details). We will call the wavelengths used in Fig. 1 (1530 nm signal and 3400 nm idler) "reference point" throughout the text.

III. EXPERIMENTAL SETUP

A simplified schematic of our experimental setup is depicted in Fig. 2. Note that only essential components are shown in Fig. 2, and components with secondary importance such as half-wave plates, alignment mirrors, and polarizing beam splitters are omitted for simplicity. In our experimental setup, we use a commercial Yb-doped fiber MLL (MenloSystems GmbH, Orange comb FC1000-250) as the pump source. It has 100 fs pulse duration Full-Width at Half-Maximum (FWHM), 250 MHz repetition rate locked to an RF source, and 10.5 W maximum output average power. The CEO_p is free running and the comb tooth linewidth (FWHM) is <200 kHz, measured at the 100 ms timescale. For the SC generation, we use an 80 cm PCF with two zero dispersion wavelengths (NKT Photonics, NL-PM-750). In order to generate the SC with the optical bandwidth shown in Fig. 1(b), our PCF required 200 mW of average pump power with a coupling efficiency of 50% (so only 100 mW reaches the PCF). The SC is optically filtered using a diffraction grating at 1530 nm with a bandwidth of 5 nm (FWHM) and combined with the CW seed laser (also set to 1530 nm) for phase-locking. See "supplementary material note 1: Supercontinuum generation" for more information. The CW seed laser is a commercial ECDL (Toptica Photonics, CTL 1550) that is locked to the SC using a PID controller (Toptica Photonics, mFALC 110) with a servo bandwidth of about 200 kHz and an RF LO (Rohde and Schwarz, SME03). In addition, all the electronic instruments used in the experiments are referenced to a 10 MHz GPS-disciplined frequency
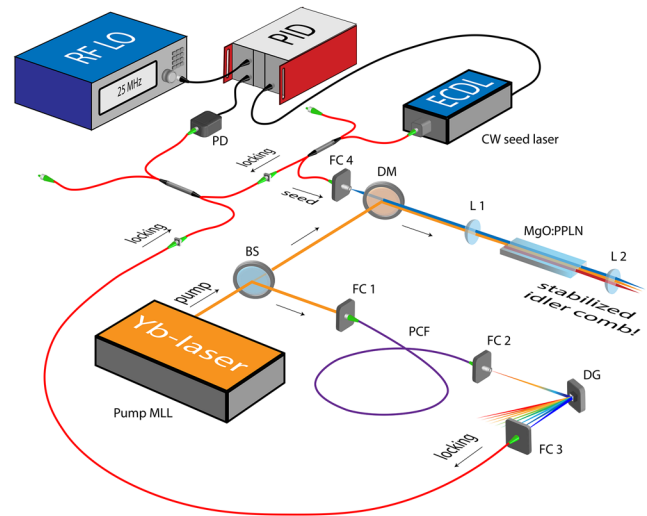
FIG. 2. Simplified experimental setup of the CW seeded OPG. The pump MLL is split into two arms: one is used to produce SC in a PCF and another is used to pump the OPG in MgO:PPLN. The output of the ECDL is split into two arms for seeding and phase-locking. The SC is optically filtered using a DG and combined with the CW seed laser to produce an RF beat note on the PD for phase-locking. Phase-locking is performed using PID and RF LO. BS: beam splitter, FC: fiber collimator, DG: diffraction grating, DM: dichroic mirror, L: lens, PD: photodiode, PID: Proportional–Integral–Derivative controller, ECDL: External Cavity Diode Laser, PCF: Photonic Crystal Fiber.

reference (MenloSystems GmbH, GPS-8), which is not shown in Fig. 2.

The MLL is used to pump a 50 mm long 5% MgO doped PPLN fanout crystal (HC Photonics) with quasi-phase-matching (QPM) periods of 26.5 μm–32.5 μm. All the interacting waves have extraordinary polarizations within the crystal. We use a focusing parameter of $\xi = 2.17$ close to the optimum 2.84 according to Boyd–Kleinman theory,[52] which resulted in 84 μm waist diameter inside the MgO:PPLN crystal. The crystal is placed in an oven with the temperature set to 75 °C to reduce the possibility of photorefractive damage. The operating wavelengths can be continuously tuned by translating the crystal in the laser beam path so that different QPM periods of the fanout structure are used. The seed CW laser beam is delivered to the OPG crystal via an optical fiber, followed by a fiber collimator for free space transfer through a dichroic mirror to the crystal. The seed laser waist size and position in the crystal are matched with those of the generated signal.

IV. RESULTS

A. Operating wavelengths, thresholds, and output powers

Figure 3(a) shows the average pump powers required to reach the OPG threshold for different operating wavelengths without seeding (red) and with 5 mW of CW seed power (blue). Due to the limited tuning range of our seed laser (1510 nm–1630 nm), we could not seed the OPG for signal wavelengths shorter than 1510 nm. At the reference point, the OPG requires 3.5 W of average pump power or 2.37 GW/cm^2 peak intensity to reach the threshold without CW
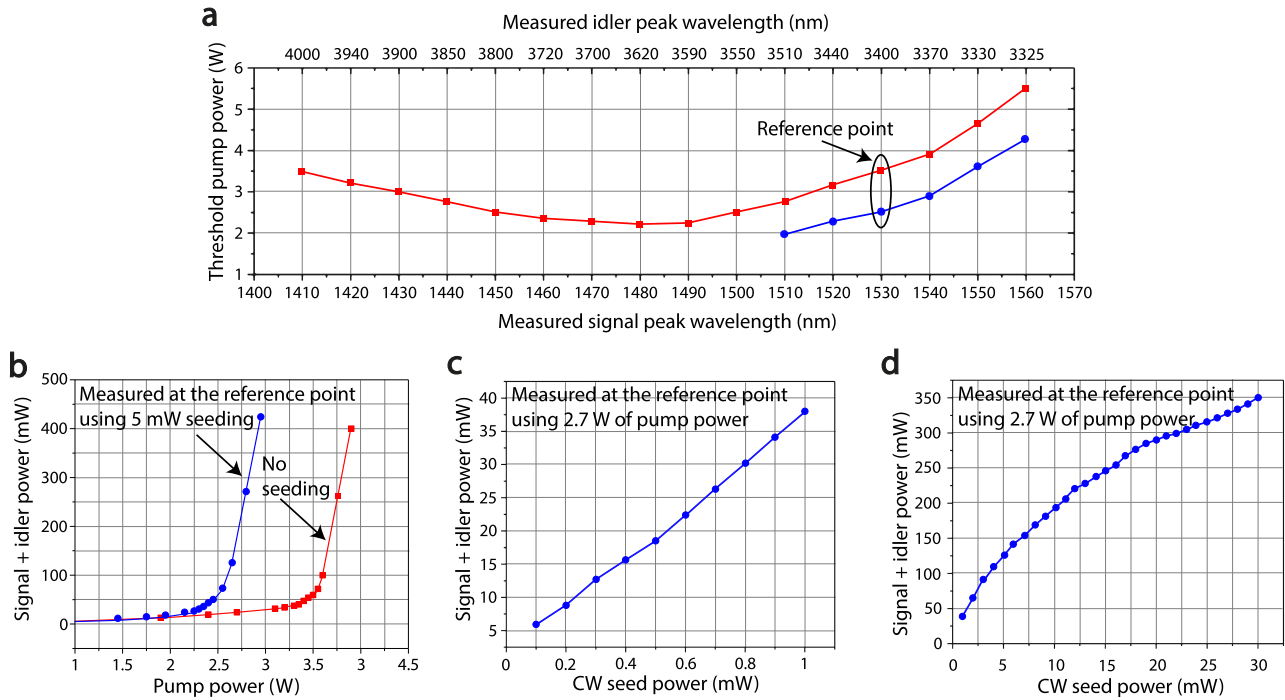
FIG. 3. OPG power measurements. (a) Input average pump power vs operating wavelengths for non-seeded OPG (red squares) and 5 mW CW seeded OPG (blue circles). Note that the threshold increases at short and long operating wavelengths because of the differences in group velocities between the pump, signal, and idler pulses. (b) Total converted power (signal + idler) for non-seeded OPG (red squares) and 5 mW CW seeded OPG (blue circles) at different average pump powers. (c) and (d) Total converted power (signal + idler, CW seed power excluded) at low and high CW seed powers, respectively, when the average pump power is fixed at 2.7 W (below the non-seeded OPG threshold).

seeding, and 2.5 W (1.69 GW/cm^2) with 5 mW CW seed power, which is about 30% threshold reduction. Corresponding threshold curves for the reference point can be seen in Fig. 3(b). Using 5.4 W (3.66 GW/cm^2) of pump power and 5 mW of seed power at the reference point, the average idler power can be as high as 700 mW (1.5 W of average signal power) with an optical bandwidth of more than 100 nm (FWHM). The resulting signal and idler optical bandwidths [~10 nm and 100 nm, respectively, see Fig. 1(d)] coincide with calculated values of phase matching bandwidths at the given poling period considering our broadband pump source. The damage threshold of our crystal was experimentally determined to be 6.8 W (4.61 GW/cm^2), above which the gray tracking effect is observed.

The effect of CW seed power on the total converted OPG power (signal + idler) is demonstrated in Figs. 3(c) and 3(d). In these measurements, the input average pump power was fixed at 2.7 W, which is below the threshold of non-seeded OPG. As can be seen in Fig. 3(c), the OPG threshold is still reached even at 100 μW of CW seed power. In addition, one can significantly increase the OPG output power by simply using higher CW seed power [see Fig. 3(d)]. Nevertheless, for the measurements described further in the text, we used 5 mW of CW seed power, which is attainable with most semiconductor lasers at the telecom wavelengths.

B. Idler CEO stability and tuning

Let us start the discussion of CEO_i stability from the CW seed laser phase-locking. Using the reference point, we first locked

the seed laser to the state governed by Eq. (3) where $\Delta f = \Delta f_{LO}$ = 25 MHz. Figure 4(a) shows the corresponding RF beat note between the seed laser and the SC when phase-locking is established. Next, we verified the phase-locking quality by measuring the double-sideband phase-noise of the beat note shown in Fig. 4(a) using the phase-detector method.[53] The integrated phase noise (100 Hz–2 MHz bandwidth) is as low as 16.5 mrad, meaning that the CW seed laser is tightly locked to the SC. In addition, we performed frequency counting of the same RF beat note. The result can be seen in Fig. 4(c) that shows the standard deviation of 34 mHz confirming high quality of phase-locking. The noise in the frequency counting experiment averages out as white noise, which is evident from the Allan deviation plot shown in Fig. 4(d). It is worth emphasizing that if one wants to make sure that the CEO_i is stabilized, the data shown in Figs. 4(a)–4(d) can be used as a reference. In order to prove this statement, we measured the CEO_i and verified its stability, which we discuss next.

The most straightforward way to determine the CEO and measure its stability is f-2f interferometry. This would require an octave spanning SC spectrum generated directly in MIR, which is a challenging task. Instead, we emulated the f-2f interferometry method by comparing the idler OFC to another OFC with a known and stabilized CEO_{ref}, which we will refer to as a reference comb. The reference comb is a commercial Er-doped fiber MLL (MenloSystems GmbH, Blue comb FC1500-250-WG) that has an inbuilt SC output spanning across 1050 nm–2100 nm, with the CEO_{ref} stabilized to 20 MHz. The reference comb does not directly overlap with the
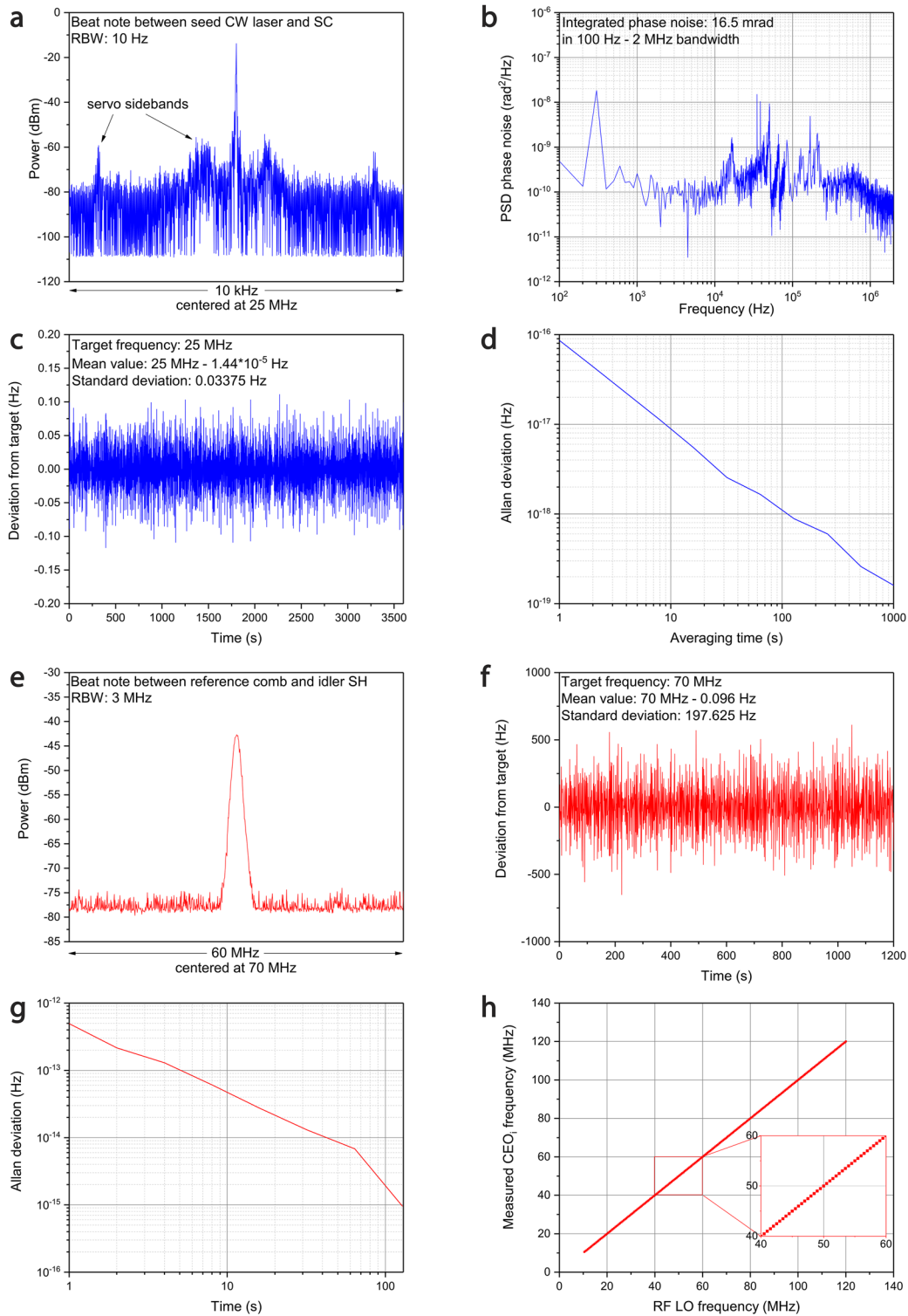
FIG. 4. CEO_i stability measurements and tuning. (a) RF beat note of the CW seed laser locked to the SC. (b) Double-sideband phase-noise (PSD) of the RF beat note [shown in (a)] when the seed laser is locked to the SC. (c) and (d) Frequency counting of the beat note shown in (a) and its Allan deviation, respectively. (e) RF beat note between the reference comb and the idler SH. (f) and (g) Frequency counting of the RF beat note shown in (e) and its Allan deviation, respectively. (h) CEO_i tuning demonstration; note that the CEO_i is continuously tunable for almost 125 MHz, which is half of the idler repetition rate.

idler comb; hence, we had to frequency double the idler comb using another MgO:PPLN crystal to produce an additional comb centered at 1700 nm. When the frequency is doubled, the CEO of the idler also doubles, meaning that the idler second harmonic (SH) offset frequency (CEO_{iSH}) is equal to twice the CEO_i. We combined the idler SH with the reference comb and set the repetition rates of both combs to 250 MHz. Using a simple delay line to overlap the optical pulses in time, we measured a single beat note with the following value:

$$f_{beat} = CEO_{ref} - CEO_{iSH} = 20 \text{ MHz} - (-2*25 \text{ MHz}) = 70 \text{ MHz}.$$

One can see a stable beat note with the expected value of 70 MHz in Fig. 4(e). It proves that the phase-locked CW seed laser transfers the instabilities of the free running CEO_p to the signal comb ($CEO_s = CEO_p + \Delta f_{LO}$), thus making the CEO_i stabilized according to Eq. (1). We used the same beat note for a frequency counting experiment that demonstrates the long term stability of CEO_i [see Fig. 4(f)]. The noise in Fig. 4(f) is limited by the mutual instability (timing jitter) between the pump comb (hence the idler comb and its SH) and the reference comb. The pump and reference combs are locked to two different RF signal generators that are both referenced to the same 10 MHz GPS-disciplined crystal oscillator. The specified relative instability of the reference oscillator is 5×10^{-12} in 1 s.

In order to demonstrate the CEO_i tuning, we swept the RF LO frequency from 10.5 MHz to 120 MHz with a step of 0.5 MHz and continuously measured the beat note frequency using an inbuilt peak finding function of the RF spectrum analyzer. The result can be seen in Fig. 4(h). As evident from the figure, the idler CEO is continuously tunable for almost half of the idler repetition rate without any interruptions. For RF LO frequencies close to 125 MHz, the phase-locking becomes unstable because the adjacent RF beat note from the next nearest comb tooth starts to overlap with the beat note under consideration. Nevertheless, when the 125 MHz point has passed, the CEO_i can be further tuned without interruptions.

C. Idler CEO modulation

Next, we modulated the RF LO frequency Δf_{LO} with a maximum modulation frequency of 20 kHz available in our RF LO. In addition, we chose the largest modulation amplitude of ± 2 MHz that allowed for stable phase-locking without changing any locking parameters of the PID controller used in the previous experiments. The corresponding RF beat notes with modulation off and on are depicted in Figs. 5(a) and 5(b) for comparison, respectively. When the modulation is on, the shape of the RF beat note is modified to the typical modulated pattern with two peaks located at the extremes of the modulation. Note that here we consider the idler SH; thus, the modulation amplitude is doubled and results in ± 4 MHz [see Fig. 5(b)]. When modulated, the central frequency of the RF beat note is precisely maintained, which would not be possible without tight phase-locking. The CEO_i modulation experiment is a good demonstration of the system's versatility. In practice, this can be used in experiments where a dynamic control of the CEO is required. For instance, one could lock the comb to an external cavity for cavity-enhanced spectroscopy, in which case both the repetition rate and CEO often need to be precisely controlled.[54] Importantly, in our method, these two parameters are independently adjustable, which is not necessarily the case with MLLs.

D. Idler linewidth and intensity noise

With regard to spectroscopy applications, there are two additional parameters of great importance—the comb tooth linewidth and the RIN. First, we estimated the comb tooth linewidth by another RF beat note measurement using an MIR CW HeNe laser (Research Electro-Optics, Model 30545) at 3390 nm. We do not have the exact information about the HeNe laser linewidth; thus, this measurement only sets an upper limit for the comb tooth linewidth. The result can be seen in Fig. 6(a) that shows an RF beat note with a 177 kHz FWHM [note the linear scale in Fig. 6(a)]. This is a narrow linewidth considering the fact that our pump MLL repetition rate is locked to an RF source, not to an ultra-stable CW-laser. The SC generation and stabilization paths as well as the linewidth measurement setup consist of mostly single mode fibers with an estimated total fiber length of 40 m. However, the additional noise added by a fiber with this length should broaden the comb tooth linewidth by less than 1 kHz.[55] Thus, this effect is not noticeable under our experimental conditions. We would also like to emphasize that all the RF
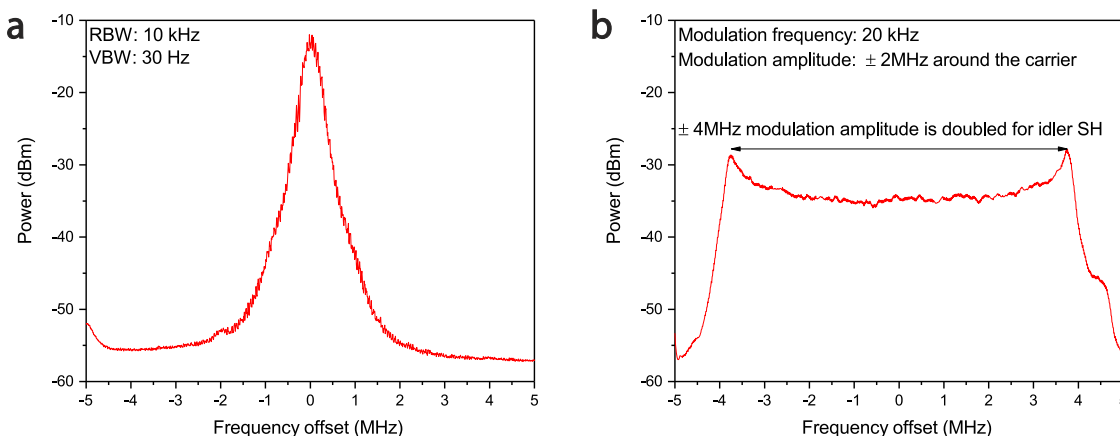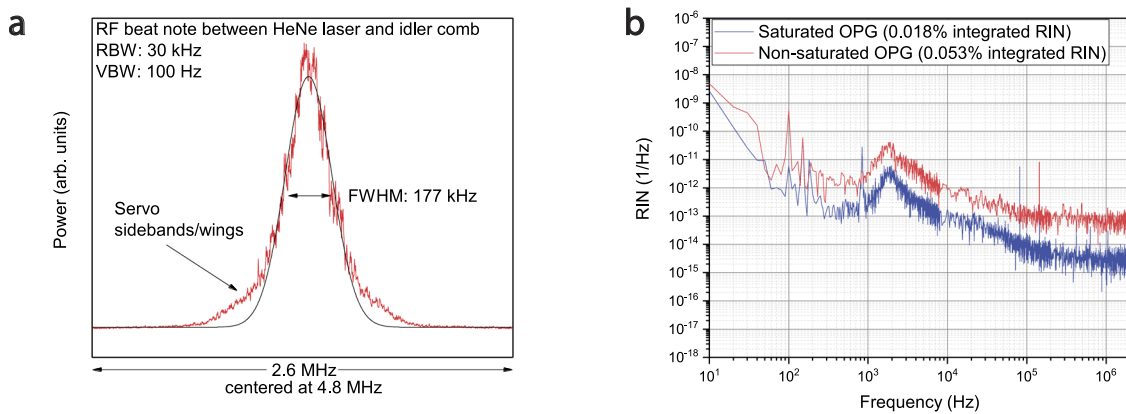
FIG. 5. Idler CEO modulation experiment. (a) and (b) RF beat note between the reference comb and the idler SH without and with modulation, respectively.

FIG. 6. Idler linewidth and RIN. (a) RF beat note between MIR HeNe laser and idler comb (red) (note the linear scale) and a Gaussian fit to the curve with servo sidebands excluded (black). (b) RIN of the idler comb in the saturated regime (blue) and non-saturated regime (red).

beat notes shown in Figs. 4(e), 5(a), and 6(a) are detectable only if the OPG is seeded by the CW source. Without CW seeding, the CEO_i is random and no RF beat note can be detected. See "supplementary material note 3: Pulse-to-pulse coherence" for more information.

The RIN measurements were performed using the reference point with two different input powers that correspond to saturated and non-saturated OPG regimes [Fig. 6(b)]. At saturation, we used an input pump power of 4.2 W that resulted in 450 mW of average output idler power. For the non-saturated regime, we used 3.2 W of average pump power that produced 170 mW of average idler power. The integrated RIN at the saturation is lower than that for the non-saturated regime; we determined it to be 0.018% and 0.053% (integrated from 10 Hz to 2 MHz) for saturated and non-saturated regimes, respectively. The result is in agreement with the theoretical predictions as well as experimental observations by another research group.[56]

V. CONCLUSIONS

We have demonstrated a simple method that allows for the generation of stabilized MIR OFCs using femtosecond OPG with CW seeding. The CW seed laser plays a key role in the method, since it establishes the idler CEO stability. Moreover, the CW seed laser makes the system highly versatile allowing one to dynamically tune and modulate the idler CEO directly in the OPG process. Our setup does not have any cavities, which means that the repetition rate can also be freely tuned. We performed all the measurements required to prove the idler CEO stability; hence, the usually challenging step of CEO determination can be omitted. An additional benefit of the scheme is its inherent insensitivity to relative timing jitter between the pump and seed, since the seed source is not pulsed. This is in contrast with DFG that relies on downshifted Raman solitons and requires a careful control of the temporal overlap between pump and signal pulses for intensity noise minimization.[57] Along with the already mentioned DFG and SPOPO methods, there are some examples of MIR OFCs that have been produced by spectral broadening in Si_3N_4[58,59] and $LiNbO_3$[60] waveguides. These systems show a great promise in the miniaturization of the MIR combs, but unfortunately the output powers are quite limited in the MIR region.

However, combining our method with nonlinear waveguide technologies could open up a new path to efficient and integrated MIR combs with dynamic CEO control.

SUPPLEMENTARY MATERIAL

See the supplementary material for details on the supercontinuum generation, phase-locking procedure, and pulse-to-pulse coherence of the described CW-seeded OPG light source.

DATA AVAILABILITY

The data that support the findings of this study are available from the corresponding authors upon reasonable request.

REFERENCES

[1]S. A. Diddams, D. J. Jones, J. Ye, S. T. Cundiff, J. L. Hall, J. K. Ranka, R. S. Windeler, R. Holzwarth, T. Udem, and T. W. Hänsch, "Direct link between microwave and optical frequencies with a 300 THz femtosecond laser comb," Phys. Rev. Lett. **84**, 5102 (2000).

[2]S. A. Diddams, J. C. Bergquist, S. R. Jefferts, and C. W. Oates, "Standards of time and frequency at the outset of the 21st century," Science **306**, 1318 (2004).

[3]H. R. Telle, G. Steinmeyer, A. E. Dunlop, J. Stenger, D. H. Sutter, and U. Keller, "Carrier-envelope offset phase control: A novel concept for absolute optical frequency measurement and ultrashort pulse generation," Appl. Phys. B **69**, 327 (1999).

[4]R. Holzwarth, T. Udem, T. W. Hänsch, J. C. Knight, W. J. Wadsworth, and P. S. J. Russell, "Optical frequency synthesizer for precision spectroscopy," Phys. Rev. Lett. **85**, 2264 (2000).

[5]T. Fortier and E. Baumann, "20 years of developments in optical frequency comb technology and applications," Commun. Phys. **2**, 153 (2019).

[6]S. A. Diddams, K. Vahala, and T. Udem, "Optical frequency combs: Coherently uniting the electromagnetic spectrum," Science **369**, eaay3676 (2020).

[7]S. A. Diddams, "The evolving optical frequency comb [Invited]," J. Opt. Soc. Am. B **27**, B51 (2010).

[8]T. Udem, R. Holzwarth, and T. W. Hänsch, "Optical frequency metrology," Nature **416**, 233 (2002).

[9]S. T. Cundiff and A. M. Weiner, "Optical arbitrary waveform generation," Nat. Photonics **4**, 760 (2010).

[10]A. Schliesser, N. Picqué, and T. W. Hänsch, "Mid-infrared frequency combs," Nat. Photonics **6**, 440 (2012).

[11]A. V. Muraviev, V. O. Smolski, Z. E. Loparo, and K. L. Vodopyanov, "Massively parallel sensing of trace molecules and their isotopologues with broadband sub-harmonic mid-infrared frequency combs," Nat. Photonics **12**, 209 (2018).

[12]M. Vainio and L. Halonen, "Mid-infrared optical parametric oscillators and frequency combs for molecular spectroscopy," Phys. Chem. Chem. Phys. **18**, 4266 (2016).

[13]L. Consolino, M. Nafa, F. Cappelli, K. Garrasi, F. P. Mezzapesa, L. Li, A. G. Davies, E. H. Linfield, M. S. Vitiello, P. De Natale, and S. Bartalini, "Fully phase-stabilized quantum cascade laser frequency comb," Nat. Commun. **10**, 2938 (2019).

[14]S. M. Foreman, D. J. Jones, and J. Ye, "Flexible and rapidly configurable femtosecond pulse generation in the mid-IR," Opt. Lett. **28**, 370 (2003).

[15]G. Krauss, D. Fehrenbacher, D. Brida, C. Riek, A. Sell, R. Huber, and A. Leitenstorfer, "All-passive phase locking of a compact Er:fiber laser system," Opt. Lett. **36**, 540 (2011).

[16]G. Soboń, T. Martynkien, P. Mergo, L. Rutkowski, and A. Foltynowicz, "High-power frequency comb source tunable from 2.7 to 4.2 μm based on difference frequency generation pumped by an Yb-doped fiber laser," Opt. Lett. **42**, 1748 (2017).

[17]T. W. Neely, T. A. Johnson, and S. A. Diddams, "High-power broadband laser source tunable from 3.0 μm to 4.4 μm based on a femtosecond Yb:fiber oscillator," Opt. Lett. **36**, 4020 (2011).

[18]S. Vasilyev, I. S. Moskalev, V. O. Smolski, J. M. Peppers, M. Mirov, A. V. Muraviev, K. Zawilski, P. G. Schunemann, S. B. Mirov, K. L. Vodopyanov, and V. P. Gapontsev, "Super-octave longwave mid-infrared coherent transients produced by optical rectification of few-cycle 2.5-μm pulses," Optica **6**, 111 (2019).

[19]A. Baltuška, T. Fuji, and T. Kobayashi, "Controlling the carrier-envelope phase of ultrashort light pulses with optical parametric amplifiers," Phys. Rev. Lett. **88**, 133901 (2002).

[20]I. Galli, F. Cappelli, P. Cancio, G. Giusfredi, D. Mazzotti, S. Bartalini, and P. De Natale, "High-coherence mid-infrared frequency comb," Opt. Express **21**, 28877 (2013).

[21]I. Galli, S. Bartalini, P. Cancio, F. Cappelli, G. Giusfredi, D. Mazzotti, N. Akikusa, M. Yamanishi, and P. De Natale, "Mid-infrared frequency comb for broadband high precision and sensitivity molecular spectroscopy," Opt. Lett. **39**, 5050 (2014).

[22]F. Adler, K. C. Cossel, M. J. Thorpe, I. Hartl, M. E. Fermann, and J. Ye, "Phase-stabilized, 1.5 W frequency comb at 2.8–4.8 μm," Opt. Lett. **34**, 1330 (2009).

[23]J. H. Sun, B. J. S. Gale, and D. T. Reid, "Composite frequency comb spanning 0.4–2.4 μm from a phase-controlled femtosecond Ti:sapphire laser and synchronously pumped optical parametric oscillator," Opt. Lett. **32**, 1414 (2007).

[24]N. Leindecker, A. Marandi, R. L. Byer, and K. L. Vodopyanov, "Broadband degenerate OPO for mid-infrared frequency comb generation," Opt. Express **19**, 6296 (2011).

[25]N. Leindecker, A. Marandi, R. L. Byer, K. L. Vodopyanov, J. Jiang, I. Hartl, M. Fermann, and P. G. Schunemann, "Octave-spanning ultrafast OPO with 2.6–6.1 μm instantaneous bandwidth pumped by femtosecond Tm-fiber laser," Opt. Express **20**, 7046 (2012).

[26]M. Vainio and J. Karhu, "Fully stabilized mid-infrared frequency comb for high-precision molecular spectroscopy," Opt. Express **25**, 4190 (2017).

[27]S. T. Wong, K. L. Vodopyanov, and R. L. Byer, "Self-phase-locked divide-by-2 optical parametric oscillator as a broadband frequency comb source," J. Opt. Soc. Am. B **27**, 876 (2010).

[28]M. Vainio and L. Halonen, "Stabilization of femtosecond optical parametric oscillators for infrared frequency comb generation," Opt. Lett. **42**, 2722 (2017).

[29]K. Hitachi, A. Ishizawa, T. Nishikawa, M. Asobe, and T. Sogawa, "Carrier-envelope offset locking with a 2f-to-3f self-referencing interferometer using a dual-pitch PPLN ridge waveguide," Opt. Express **22**, 1629 (2014).

[30]M. J. Thorpe, D. Balslev-Clausen, M. S. Kirchner, and J. Ye, "Cavity-enhanced optical frequency comb spectroscopy: Application to human breath analysis," Opt. Express **16**, 2387 (2008).

[31]F. Keilmann, C. Gohle, and R. Holzwarth, "Time-domain mid-infrared frequency-comb spectrometer," Opt. Lett. **29**, 1542 (2004).

[32]I. Coddington, N. Newbury, and W. Swann, "Dual-comb spectroscopy," Optica **3**, 414 (2016).

[33]G. Ycas, F. R. Giorgetta, E. Baumann, I. Coddington, D. Herman, S. A. Diddams, and N. R. Newbury, "High-coherence mid-infrared dual-comb spectroscopy spanning 2.6 to 5.2 μm," Nat. Photonics **12**, 202 (2018).

[34]I. Galli, S. Bartalini, S. Borri, P. Cancio, D. Mazzotti, P. De Natale, and G. Giusfredi, "Molecular gas sensing below parts per trillion: Radiocarbon-dioxide optical detection," Phys. Rev. Lett. **107**, 270802 (2011).

[35]M. Vainio, M. Merimaa, and L. Halonen, "Frequency-comb-referenced molecular spectroscopy in the mid-infrared region," Opt. Lett. **36**, 4122 (2011).

[36]A. Baltuška, T. Udem, M. Uiberacker, M. Hentschel, E. Goulielmakis, C. Gohle, R. Holzwarth, V. S. Yakovlev, A. Scrinzi, T. W. Hänsch, and F. Krausz, "Attosecond control of electronic processes by intense light fields," Nature **421**, 611 (2003).

[37]G. M. Rossi, R. E. Mainz, Y. Yang, F. Scheiba, M. A. Silva-Toledo, S.-H. Chia, P. D. Keathley, S. Fang, O. D. Mücke, C. Manzoni, G. Cerullo, G. Cirmi, and F. X. Kärtner, "Sub-cycle millijoule-level parametric waveform synthesizer for attosecond science," Nat. Photonics **14**, 629 (2020).

[38]A. Marandi, K. A. Ingold, M. Jankowski, and R. L. Byer, "Cascaded half-harmonic generation of femtosecond frequency combs in the mid-infrared," Optica **3**, 324 (2016).

[39]J. Karhu, T. Tomberg, F. Senna Vieira, G. Genoud, V. Hänninen, M. Vainio, M. Metsälä, T. Hieta, S. Bell, and L. Halonen, "Broadband photoacoustic spectroscopy of ^{14}CH$_4$ with a high-power mid-infrared optical frequency comb," Opt. Lett. **44**, 1142 (2019).

[40]J. T. Friedlein, E. Baumann, K. A. Briggman, G. M. Colacion, F. R. Giorgetta, A. M. Goldfain, D. I. Herman, E. V. Hoenig, J. Hwang, N. R. Newbury, E. F. Perez, C. S. Yung, I. Coddington, and K. C. Cossel, "Dual-comb photoacoustic spectroscopy," Nat. Commun. **11**, 3152 (2020).

[41]T. Tomberg, A. Muraviev, Q. Ru, and K. L. Vodopyanov, "Background-free broadband absorption spectroscopy based on interferometric suppression with a sign-inverted waveform," Optica **6**, 147 (2019).

[42]B. Köhler, U. Bäder, A. Nebel, J.-P. Meyn, and R. Wallenstein, "A 9.5-W 82-MHz-repetition-rate picosecond optical parametric generator with CW diode laser injection seeding," Appl. Phys. B **75**, 31 (2002).

[43]W. Chen, J. Fan, A. Ge, H. Song, Y. Song, B. Liu, L. Chai, C. Wang, and M. Hu, "Intensity and temporal noise characteristics in femtosecond optical parametric amplifiers," Opt. Express **25**, 31263 (2017).

[44]C. Gu, Z. Zuo, D. Luo, Z. Deng, Y. Liu, M. Hu, and W. Li, "Passive coherent dual-comb spectroscopy based on optical-optical modulation with free running lasers," PhotoniX **1**, 7 (2020).

[45]S. Hädrich, T. Gottschall, J. Rothhardt, J. Limpert, and A. Tünnermann, "CW seeded optical parametric amplifier providing wavelength and pulse duration tunable nearly transform limited pulses," Opt. Express **18**, 3158 (2010).

[46]M. Tiihonen, V. Pasiskevicius, A. Fragemann, C. Canalias, and F. Laurell, "Ultrabroad gain in an optical parametric generator with periodically poled KTiOPO$_4$," Appl. Phys. B **85**, 73 (2006).

[47]P. S. Kuo, K. L. Vodopyanov, M. M. Fejer, D. M. Simanovskii, X. Yu, J. S. Harris, D. Bliss, and D. Weyburne, "Optical parametric generation of a mid-infrared continuum in orientation-patterned GaAs," Opt. Lett. **31**, 71 (2006).

[48]M. Levenius, V. Pasiskevicius, F. Laurell, and K. Gallo, "Ultra-broadband optical parametric generation in periodically poled stoichiometric LiTaO$_3$," Opt. Express **19**, 4121 (2011).

[49]H. Linnenbank and S. Linden, "High repetition rate femtosecond double pass optical parametric generator with more than 2 W tunable output in the NIR," Opt. Express **22**, 18072 (2014).

[50] A. Aadhi and G. K. Samanta, "High power, high repetition rate, tunable broadband mid-IR source based on single-pass optical parametric generation of a femtosecond laser," Opt. Lett. **42**, 2886 (2017).

[51] C. Manzoni, G. Cirmi, D. Brida, S. De Silvestri, and G. Cerullo, "Optical-parametric-generation process driven by femtosecond pulses: Timing and carrier-envelope phase properties," Phys. Rev. A **79**, 033818 (2009).

[52] G. D. Boyd and D. A. Kleinman, "Parametric interaction of focused Gaussian light beams," J. Appl. Phys. **39**, 3597 (1968).

[53] R. P. Scott, C. Langrock, and B. H. Kolner, "High-dynamic-range laser amplitude and phase noise measurement techniques," IEEE J. Sel. Top. Quantum Electron. **7**, 641 (2001).

[54] F. Adler, M. J. Thorpe, K. C. Cossel, and J. Ye, "Cavity-enhanced direct frequency comb spectroscopy: Technology and applications," Annu. Rev. Anal. Chem. **3**, 175 (2010).

[55] L.-S. Ma, P. Jungner, J. Ye, and J. L. Hall, "Delivering the same optical frequency at two places: Accurate cancellation of phase noise introduced by an optical fiber or other time-varying path," Opt. Lett. **19**, 1777 (1994).

[56] J. Fan, W. Chen, C. Gu, Y. Song, L. Chai, C. Wang, and M. Hu, "Noise characteristics of high power fiber-laser pumped femtosecond optical parametric generation," Opt. Express **25**, 24594 (2017).

[57] V. Silva de Oliveira, A. Ruehl, P. Masłowski, and I. Hartl, "Intensity noise optimization of a mid-infrared frequency comb difference-frequency generation source," Opt. Lett. **45**, 1914 (2020).

[58] B. Kuyken, T. Ideguchi, S. Holzner, M. Yan, T. W. Hänsch, J. Van Campenhout, P. Verheyen, S. Coen, F. Leo, R. Baets, G. Roelkens, and N. Picqué, "An octave-spanning mid-infrared frequency comb generated in a silicon nanophotonic wire waveguide," Nat. Commun. **6**, 6310 (2015).

[59] H. Guo, C. Herkommer, A. Billat, D. Grassani, C. Zhang, M. H. P. Pfeiffer, W. Weng, C.-S. Brès, and T. J. Kippenberg, "Mid-infrared frequency comb via coherent dispersive wave generation in silicon nitride nanophotonic waveguides," Nat. Photonics **12**, 330 (2018).

[60] A. S. Kowligy, A. Lind, D. D. Hickstein, D. R. Carlson, H. Timmers, N. Nader, F. C. Cruz, G. Ycas, S. B. Papp, and S. A. Diddams, "Mid-infrared frequency comb generation via cascaded quadratic nonlinearities in quasi-phase-matched waveguides," Opt. Lett. **43**, 1678 (2018).